International Journal of Hydrogen Energy 140 (2025) 473–482

Contents lists available at ScienceDirect

International Journal of Hydrogen Energy

journal homepage: www.elsevier.com/locate/he

Passivity-based control for methane steam reforming in nuclear cogeneration systems

Junyi Li *, Zhe Dong **

Institute of Nuclear and New Energy Technology (INET), Collaborative Innovation Center of Advanced Nuclear Energy Technology of China, Key Laboratory of Advanced Reactor Engineering and Safety of Ministry of Education, Tsinghua University, Beijing, 100084, China

ARTICLE INFO

Handling Editor: Dr M Mahdi Najafpour

Keywords:
Passivity-based control
Methane steam reforming
Nuclear cogeneration

ABSTRACT

This paper presents a passivity-based control design for methane steam reforming reactors, focusing on ensuring system stability and improving dynamic performance. A deviation-based dynamic model is developed for control design, incorporating thermodynamic properties to achieve energy-efficient regulation. The proposed passivity-based control framework leverages entropy production metrics and a carefully constructed storage function to assess and ensure the system's passivity. The control design guarantees the negative definiteness of the rate of change of the storage function along the closed-loop system dynamics, and is applied to a hydrogen production plant in a nuclear cogeneration system to verify the control design. Simulation results demonstrate the effectiveness of the PBC approach in maintaining reformer stability and enhancing operational efficiency under varying disturbances.

Nomenclature

Abbreviations	
AF	Availability function
ANN	Artificial neural network
CSTR	Continuous stirred tank reactor
MPC	Model predictive control
mHTGR	Modular high-temperature gas-cooled reactor
MSR	Methane steam reforming
NSSS	Nuclear steam supply system
PBC	Passivity-based control
PH	Port Hamiltonian
PI	Proportional-integral
RNN	Recurrent neural network
ROC	Rate of change
Symbols	
A_k	Pre-exponential factor of the reaction rate coefficient
c_p	Isobaric specific heat capacity
c_v	Isochoric specific heat capacity
e	Specific internal energy
E_a	Activation energy of the reaction
K_{eq}	Reaction equilibrium constant
k_f	Forward reaction rate constant
k_r	Reverse reaction rate constant
M_i	Molar mass of species i
$\dot{n}_i$	Molar flow rate of species i
N_i	Mole number of species i
P	Pressure
Q	External heat
r_{rxn}	Reaction rate
s	Specific entropy
T	Temperature
v	Specific volume
V	Volume of reactor
ΔH_{rxn}	Enthalpy of reaction
ε	Entropy production metric
μ_i	Chemical potential of species i
ν_i	Signed stoichiometric coefficient of species i
τ	Residence time
χ	Isothermal compressibility factor

1. Introduction

Hydrogen, as an environmentally friendly alternative fuel, has the highest energy content per unit mass compared to conventional fuels [1, 2]. The global demand for hydrogen energy is expected to increase by about 400 Mt/year in the next 50 years. Methane steam reforming (MSR) is the key process in hydrogen production. It accounts for about half of the total hydrogen production globally, serving as an essential

* Corresponding author.
** Corresponding author.
E-mail addresses: lijunyi20@mails.tsinghua.edu.cn (J. Li), dongzhe@mail.tsinghua.edu.cn (Z. Dong).

https://doi.org/10.1016/j.ijhydene.2025.05.367
Received 10 February 2025; Received in revised form 22 May 2025; Accepted 26 May 2025
Available online 30 May 2025

pathway toward sustainable energy system [3]. The process produces hydrogen gas by reacting methane and steam at high-temperature in the presence of catalysts. The MSR reactor, often denoted as a reformer, is the critical component of the process, exhibiting highly nonlinear and complex dynamic behaviors due to the interactions of chemical reactions, heat transfer, and mass flows. Recent advancements in control strategies have leveraged both classical and data-driven approaches to optimize performance, stability, and energy efficiency.

Proportional-integral (PI) controllers, often enhanced with advanced techniques such as neural networks, have been widely employed in MSR systems to maintain desired process variables, such as hydrogen production rates and methane conversion rates. For instance, a PI-based hybrid control strategy has been proposed, which integrates a back-propagation neural network optimized by genetic algorithms to form a feedforward-feedback system for regulating inlet flow rates in reactors [4]. A computational fluid dynamics model of an industrial-scale reformer is developed and proportional, PI, and optimization-integral feedback control schemes are evaluated, demonstrating their effectiveness in driving the hydrogen mole fraction at the tube outlet to a desired set point under feed disturbances, significantly improving process dynamics compared to open-loop control [5]. The reformer complex dynamics are reduced to decoupled linear subsystems easily controllable using PI linear control by using two nested control loops: the inner loop compensates for nonlinear cross-coupling using static nonlinear feedback, while the outer loop, based on an extended state observer, estimates and compensates modeling errors [6].

Despite their widespread use, these methods often struggle to handle the inherent nonlinearities and coupled dynamics of MSR processes. Model Predictive Control (MPC) has been developed to handle nonlinearities in MSR processes. A gain-scheduled model predictive control system for steam methane reformers is introduced to optimize critical process parameters, such as outlet methane concentration and reformed gas temperature, demonstrating superior performance over PID controllers, including better disturbance rejection and safe operation within thermal constraints [7].

Data-driven control models have emerged as promising tools for addressing the challenges in MSR control. Artificial neural networks (ANNs), particularly recurrent neural networks (RNNs), have been employed to model nonlinear process dynamics using time-series data. For example, an ANN-based predictive model trained on extensive operational data demonstrated high accuracy in predicting key variables, such as syngas flow rate and hydrogen composition, enabling optimized control and improved process efficiency [8]. By leveraging data preprocessing, hyperparameter tuning, and predictive modeling, an ANN-based control-oriented model is developed to optimize the MSR process, define the optimal operating conditions, and improve process efficiency [9].

Traditional reformers are heated by furnaces that burn a portion of the process feedstock to provide the high temperatures required for the endothermic reaction. Alternative heating methods for the reformer, such as electrically heated and solar-driven systems, are increasingly being explored for their potential to reduce greenhouse gas emissions and improve energy efficiency [10,11]. Advanced control strategies for these reformers have also been developed to ensure reliable operation under these new heating approaches. Electrification introduces precise thermal management challenges, which have been addressed by integrating experimental data and using MPC [12] and extended Luenberger observer-based MPC [13]. These systems integrate dynamic models with real-time feedback to optimize temperature profiles and ensure stable operation. Similarly, hybrid control strategies combining neural networks and classical controllers have been implemented to mitigate the effects of radiation fluctuations, achieving stable operation and enhanced transient performance under variable solar radiation conditions [14]. The effectiveness of long short-term memory-based RNN models in enhancing MPC for electrically heated MSR processes has been demonstrated, particularly in handling disturbances and process variability through strategies like real-time retraining and offset-free MPC [15].

While classical and data-driven control strategies have demonstrated their effectiveness in addressing the challenges of MSR, they often rely on specific modeling assumptions or significant computational resources. These limitations highlight the need for alternative approaches that leverage the inherent physical properties of the system, such as energy dissipation and stability. PBC emerges as a promising framework in this context, offering robust performance by directly exploiting the process passivity characteristics. By constructing a storage function grounded in thermodynamic properties, PBC ensures energy dissipation, leading to stable performance without requiring computationally intensive optimization.

The use of thermodynamic availability as a storage function for PBC design has been explored to ensure the stability of single-phase reactive systems with chemical equilibrium [16]. The approach was applied to a reformer, showcasing the control of pressure and temperature using passive input-output mappings. Nonlinear state feedback control laws have been developed for stabilizing non-isothermal tubular reactors modeled by nonlinear partial differential equations, with thermodynamic availability and reduced availability functions serving as Lyapunov candidates [17]. The availability function derived from the entropy concavity has been emplyed as a Lyapunov function for stability analysis and control design of non-isothermal Continuous Stirred Tank Reactors (CSTRs), with applications shown in both open-loop stability assessment and closed-loop control [18]. The study also develops a thermodynamic availability function as a storage function for feedback control and demonstrates its application to gas-phase equilibrium reactors.

The port Hamiltonian (PH) framework provides a powerful mathematical structure for modeling and controlling physical systems by representing energy exchanges and dissipation in a structured and thermodynamically consistent manner [19–21]. One study employs a passivity-based approach within the PH framework to design a nonlinear controller for stabilizing non-isothermal CSTRs around desired stationary points, incorporating asymptotic observers for systems with incomplete state measurements [22].

Irreversible PH systems are combined with the thermodynamic availability function to propose a PBC framework for irreversible processes in Ref. [23]. This approach ensures thermodynamically coherent closed-loop behavior by leveraging energy-shaping techniques to stabilize temperature and pressure in gas-phase equilibrium reactors. Further, a thermodynamical pseudo-Hamiltonian formulation of the CSTR model has been proposed for both isothermal and non-isothermal cases. In this study, the Interconnection and Damping Assignment PBC method is applied, where the closed-loop Hamiltonian function is proportional to the thermodynamic availability function [24]. Passivity-based inventory control has been integrated into the port-Hamiltonian (PH) framework by employing inventory-related storage functions as the closed-loop Hamiltonian, thereby enabling the design of feedback laws that achieve global and exponential stabilization of chemically reacting systems [25]. An extended-state PBC approach has been proposed for thermodynamic systems within the PH framework and entropy production metrics, incorporating entropy production metrics to ensure asymptotic stability and minimize entropy production at steady state [26].

Passivity theory provides a robust framework for handling nonlinearity and feedback stability in dynamic systems. Combining passivity with thermodynamic properties enables a systematic approach to address challenges in chemical reactors operating near equilibrium. Current PBC methods have shown promise in stabilizing chemical reactors, however, their application to MSR reactors, which mainly are fixed-bed reactors, remains little explored.

This paper proposes a PBC design for MSR reactors. The control design is based on ensuring the passivity of the system by defining a suitable storage function and giving control design that guarantee negative definiteness. By utilizing a deviation-based model that captures

system dynamics relative to a desired equilibrium, a storage function using entropy production metric is given, and corresponding control laws are designed. In contrast to prior approaches that rely on availability functions, the entropy production-based storage function directly reflects the system's irreversible thermodynamic behavior and internal dissipation. This enables a more physically grounded formulation of the passivity condition, especially suitable for chemical systems with strong nonlinearities and non-equilibrium effects.

The practical significance of this work is demonstrated through application to a hydrogen production plant in a nuclear cogeneration system based on the modular high-temperature gas-cooled reactor (mHTGR). Using the abundant and consistent heat from nuclear reactors, this approach enhances the overall efficiency and sustainability of the hydrogen production process [27,28]. The mHTGR is a small modular reactor with inherent safety advantages, and its nuclear steam supply system (NSSS) can provide steam at around 560 °C. The MSR hydrogen production system uses an electrical heater to further heat the steam from the NSSSs to a higher temperature. This heated steam is then used to provide reaction heat for the reformer. After heating the reformer, the steam remains at high temperatures and is sent to the turbine sets for electricity generation. This configuration not only reduces carbon emissions but also provides a stable, continuous heat source, making it highly suitable for large-scale hydrogen production. The coupling of MSR with NSSS necessitates advanced control strategies capable of maintaining operational stability and efficiency while addressing disturbances arising from fluctuations in reactor output or process demand.

2. Passivity-based control approach

To address the control challenges associated with the MSR reactor, a PBC framework is adopted. The PBC approach leverages the system's inherent energy properties to ensure stability and facilitate controller design by representing the dynamics in a PH form. In this context, establishing an appropriate system formulation and identifying a suitable storage function are essential for analyzing passivity and deriving stability conditions.

2.1. State-space model for control design

Consider a chemical reactor involving a chemical reaction with n_c active component, characterized by the following reaction invariant, $\sum_i^{n_c} \nu_i M_i = 0$,

$$\sum_i^{n_c} \nu_i M_i = 0, \tag{1}$$

where ν_i and M_i are respectively the signed stoichiometric coefficient and the molar mass of species i as it enters the reactor. If species i is consumed in the reaction, then $\nu_i < 0$; conversely, $\nu_i > 0$ if species i is produced.

The following assumptions are made.

(1) At the inlet of the reactor, the components i are fed at fixed temperature T_{in};
(2) The reactor is isobaric and the mixture is ideal.
(3) The total reaction rate is expressed as

$$r_{\text{rxn}} = r^f_{\text{rxn}} - r^r_{\text{rxn}}, \tag{2}$$

where r^f_{rxn} and r^r_{rxn} are the forward and reverse reaction rates respectively, and they can be expressed using the rate constants and the concentration of the species i, denoted as $[i]$, as follows,

$$\begin{cases} r^f_{\text{rxn}} = k_f(T) \prod\limits_{i \in reactants} [i]^{|\nu_i|}, \\ r^r_{\text{rxn}} = k_r(T) \prod\limits_{i \in products} [i]^{|\nu_i|}, \end{cases} \tag{3}$$

where k_f and k_r is the forward and reverse reaction rate constant given by the Arrhenius equation,

$$k(T) = A_k \, exp\left(-\frac{E_a}{RT}\right), \tag{4}$$

where A_k is the pre-exponential factor of the reaction rate coefficient, E_a is the energy activation of the reaction, T is the reaction temperature. The reaction rate describes the rate at which the concentration of reactants changes over time. At equilibrium, the forward reaction rate equals to the reverse reaction rate, resulting in constant concentration for all species in the chemical reactor, and the equilibrium constant is given by

$$K_{\text{eq}}(T) = k_f(T)/k_r(T). \tag{5}$$

A continuous chemical reactor with volume V, is fed at a constant temperature T_{in}. The material balance is given as follows,

$$\dot{N}_i = \dot{n}_{i,\text{in}} - \dot{n}_{i,\text{out}} + \nu_i r_{\text{rxn}} V, \tag{6}$$

where N_i and $\dot{n}_i$ are the total number of mole and the molar flow rate of species i respectively, the outlet flow rate of species i is given as

$$\dot{n}_{i,\text{out}} = N_i/\tau, \tag{7}$$

where τ is the residence time describing the average amount of time the substance spends in the reactor.

The energy balance for a chemical reactor can be expressed as,

$$C_{\text{p}}\dot{T} = G_{\text{f}}\left(c_{\text{p,in}} T_{\text{in}} - c_{\text{p}} T\right) - \Delta H_{\text{rxn}} r_{\text{rxn}} V + \dot{Q}, \tag{8}$$

where ΔH_{rxn} is the reaction enthalpy, $\dot{Q}$ is the external heat supplied to the chemical reactor, where C_{p} is the total heat capacity of the reactor, G_{f} is the mass flow rate at the outlet of the reactor, $c_{\text{p,in}}$ is the specific heat capacity of the reactants at the inlet. Define $C_{\text{fin}} = G_{\text{f}} c_{\text{p,in}}$ and $C_{\text{f}} = G_{\text{f}} c_{\text{p}}$, (8) can be written as

$$C_{\text{p}}\dot{T} = C_{\text{fin}} T_{\text{in}} - C_{\text{f}} T - \Delta H_{\text{rxn}} r_{\text{rxn}} V + \dot{Q}. \tag{9}$$

In summary, the dynamics of a chemical reactor can be represented as

$$\begin{cases} \dot{N}_i = \dot{n}_{i,\text{in}} - N_i/\tau + \nu_i r_{\text{rxn}} V, \\ \dot{T} = C_{\text{fin}} T_{\text{in}}/C_{\text{p}} - C_{\text{f}} T/C_{\text{p}} - \Delta H_{\text{rxn}} r_{\text{rxn}} V/C_{\text{p}} + \dot{Q}/C_{\text{p}}. \end{cases} \tag{10}$$

Let the steady-state operating point be denoted by N_{i0}, T_0, $\dot{n}_{i,\text{in}0}$ and $\dot{Q}_0$, the deviation state vector is defined as

$$\begin{cases} \delta N_i = N_i - N_{i0}, \\ \delta T = T - T_0, \end{cases} \tag{11}$$

and the control input vector be defined as

$$\begin{cases} \delta \dot{n}_{i,\text{in}0} = \dot{n}_{i,\text{in}} - \dot{n}_{i,\text{in}0}, \\ \delta \dot{Q} = \dot{Q} - \dot{Q}_0, \end{cases} \tag{12}$$

Consider a nonlinear state-space model with the dynamics (10) with control input $\boldsymbol{u}$ shown as

$$\dot{\boldsymbol{x}} = \boldsymbol{f}(\boldsymbol{x}) + \boldsymbol{G}(\boldsymbol{x})\boldsymbol{u}, \tag{13}$$

where $\boldsymbol{x} = [\,\delta \boldsymbol{N} \quad \delta T\,]^{\text{T}}$ is the state vector, $\boldsymbol{f}(\boldsymbol{x}) \in \mathbb{R}^n$ is the drift vector, $\boldsymbol{G}(\boldsymbol{x}) \in \mathbb{R}^{n \times m}$ is the input-state map with control inputs $\boldsymbol{u} = [\,\delta \dot{\boldsymbol{n}}_{\text{in}} \quad \delta \dot{Q}\,]^{\text{T}}$.

2.2. Storage function

The entropy production metric ε [26] for irreversible systems is defined as,

$$\delta\varepsilon = s\delta T - v\delta P + \sum_i N_i \delta\mu_i, \tag{14}$$

where s is the specific entropy, v is the specific volume, e is the specific internal energy, P is the pressure, N_i and μ_i are the mole number and chemical potential of the ith species, respectively. The operator δ represents first-order deviations of physical variables. $\delta\varepsilon$ equals to zero at steady states.

Its second-order deviation $\delta^2\varepsilon$ satisfies

$$\delta^2\varepsilon = \frac{c_v}{T}(\delta T)^2 + \frac{1}{\chi v}(\delta v)^2_{\{N_i\}} + \sum_{i,j}\left(\frac{\partial \mu_i}{\partial N_j}\right)_{p,T,(N_j)} \delta N_i \delta N_j, \tag{15}$$

where

$$(\delta v)_{\{N_i\}} = \left(\frac{\partial v}{\partial T}\right)_{P,\{N_i\}} \delta T + \left(\frac{\partial v}{\partial p}\right)_{T,\{N_i\}} \delta P, \tag{16}$$

for $\{N_i\}$ means that N_i is given for all i, while (N_i) stands for that n_k is given when $k \neq i$, and c_v is the isochoric specific heat capacity. The isothermal compressibility factor of working fluids is given by

$$\chi = -\frac{1}{v}\left(\frac{\partial v}{\partial P}\right)_{T,\{N_i\}}. \tag{17}$$

When the following inequalities are satisfied,

$$c_v > 0, \tag{18}$$

$$\boldsymbol{U} := \left[\mu_{ij}\right] > \boldsymbol{O}, \tag{19}$$

and

$$\chi > 0, \tag{20}$$

$\delta^2\varepsilon$ is strictly positive definite, implying that the entropy production ε reaches a local minimum at steady state, where

$$\mu_{ij} = \left(\frac{\partial \mu_i}{\partial N_j}\right)_{P,T,(N_j)}. \tag{21}$$

These conditions were proven in Ref. [26] and are directly adopted here. For completeness, the proof of these conditions is presented in Appendix A.1. Since $\delta^2\varepsilon$ is strictly positive definite under conditions (18)–(20), it is suitable to choose the storage function in thermodynamic systems as

$$H(\boldsymbol{x}) = \frac{1}{2}\delta^2\varepsilon(\boldsymbol{x}). \tag{22}$$

From (15), the entropy production metric due to the chemical reaction is

$$\delta^2\varepsilon_c(x_1, x_2, x_3, x_4) = \sum_{i,j}\left(\frac{\partial \mu_i}{\partial N_j}\right)_{P,T,(N_j)} \delta N_i \delta N_j = \boldsymbol{x}_c^{\mathrm{T}} \boldsymbol{U} \boldsymbol{x}_c, \tag{23}$$

where $\boldsymbol{x}_c = [x_1 \quad x_2 \quad x_3 \quad x_4]^{\mathrm{T}}$.

For the entropy production metric due to heat transfer, the entropy production metric is

$$\delta^2\varepsilon_h(x_5) = \frac{c_v}{T}(\delta T)^2 = \frac{c_v}{T}x_5^2. \tag{24}$$

Since the entropy production metric is an extensive quantity, the entropy production metric of the MSR reactor is the sum of the entropy production metric due to the chemical reaction and heat transfer, shown as

$$\delta^2\varepsilon(\boldsymbol{x}) = \delta^2\varepsilon_c(x_1, x_2, x_3, x_4) + \delta^2\varepsilon_h(x_5) = \boldsymbol{x}_c^{\mathrm{T}}\boldsymbol{U}\boldsymbol{x}_c + \frac{c_v}{T}x_5^2. \tag{25}$$

When conditions (18)–(20) are satisfied, (22) can be employed as the storage function of the chemical reactor.

2.3. Port-Hamiltonian form of the chemical reactor dynamics

Consider the nonlinear state-space model (13), since the deviations are used as state variables, the origin $\boldsymbol{x} = 0$ represents the expected steady-state point of the system, and $f(\boldsymbol{x})$ satisfies

$$\boldsymbol{f}(\boldsymbol{O}) = \boldsymbol{O}. \tag{26}$$

Following the result established in Ref. [26], if the system's storage function is chosen as (22) and $\delta^2\varepsilon$ is strictly positive definite, then there exists a structure matrix $\boldsymbol{M}(\boldsymbol{x}) \in \mathrm{R}^{n\times n}$ such that

$$\boldsymbol{M}(\boldsymbol{x})\nabla H(\boldsymbol{x}) = \boldsymbol{f}(\boldsymbol{x}), \tag{27}$$

and the system dynamics (13) can be equivalently expressed in the PH form as follow

$$\dot{\boldsymbol{x}} = [\boldsymbol{J}(\boldsymbol{x}) - \boldsymbol{R}(\boldsymbol{x})]\nabla H(\boldsymbol{x}) + \boldsymbol{G}(\boldsymbol{x})\boldsymbol{u}, \tag{28}$$

where the gradient of the storage function is defined as

$$\nabla H(\boldsymbol{x}) = \frac{\partial H(\boldsymbol{x})}{\partial \boldsymbol{x}}, \tag{29}$$

and the structure and dissipation matrices are constructed as

$$\boldsymbol{J}(\boldsymbol{x}) = \frac{1}{2}\left[\boldsymbol{M}(\boldsymbol{x}) - \boldsymbol{M}^{\mathrm{T}}(\boldsymbol{x})\right] = -\boldsymbol{J}^{\mathrm{T}}(\boldsymbol{x}), \tag{30}$$

$$\boldsymbol{R}(\boldsymbol{x}) = -\frac{1}{2}\left[\boldsymbol{M}(\boldsymbol{x}) + \boldsymbol{M}^{\mathrm{T}}(\boldsymbol{x})\right] = \boldsymbol{R}^{\mathrm{T}}(\boldsymbol{x}). \tag{31}$$

For a system described in the PH form (28), the rate of change (ROC) of the storage function $H(\boldsymbol{x})$ along the system trajectories satisfies

$$\begin{aligned}\dot{H}(\boldsymbol{x}) &= \nabla H(\boldsymbol{x})^{\mathrm{T}}\dot{\boldsymbol{x}} = \nabla H(\boldsymbol{x})^{\mathrm{T}}[\boldsymbol{J}(\boldsymbol{x}) - \boldsymbol{R}(\boldsymbol{x})]\nabla H(\boldsymbol{x}) + \nabla H(\boldsymbol{x})^{\mathrm{T}}\boldsymbol{G}(\boldsymbol{x})\boldsymbol{u} \\ &= -\nabla H(\boldsymbol{x})^{\mathrm{T}}\boldsymbol{R}(\boldsymbol{x})\nabla H(\boldsymbol{x}) + \nabla H(\boldsymbol{x})^{\mathrm{T}}\boldsymbol{G}(\boldsymbol{x})\boldsymbol{u}.\end{aligned} \tag{32}$$

Define the output as

$$\boldsymbol{y} = \boldsymbol{G}(\boldsymbol{x})^{\mathrm{T}}\nabla H(\boldsymbol{x}), \tag{33}$$

then

$$\dot{H}(\boldsymbol{x}) = -\nabla H(\boldsymbol{x})^{\mathrm{T}}\boldsymbol{R}(\boldsymbol{x})\nabla H(\boldsymbol{x}) + \boldsymbol{u}^{\mathrm{T}}\boldsymbol{y}. \tag{34}$$

If $\boldsymbol{R}(\boldsymbol{x})$ is non-negative definite, the following inequality holds

$$\dot{H}(\boldsymbol{x}) \leq \boldsymbol{u}^{\mathrm{T}}\boldsymbol{y}, \tag{35}$$

which indicates that the system is passive. Passivity implies that the system does not generate energy on its own, and the net energy supplied from the environment is either dissipated or accumulated as internal energy within the system.

Remark 1. In the absence of external inputs, i.e., $\boldsymbol{u} = \boldsymbol{0}$, the inequality reduces the following equation,

$$\dot{H}(\boldsymbol{x}) = -\nabla H(\boldsymbol{x})^{\mathrm{T}}\boldsymbol{R}(\boldsymbol{x})\nabla H(\boldsymbol{x}), \tag{36}$$

when the following conditions are satisfied

$$\begin{cases}\boldsymbol{R} \geq \boldsymbol{O}, \\ \left\{\nabla H(\boldsymbol{x})^{\mathrm{T}}\boldsymbol{R}(\boldsymbol{x})\nabla H(\boldsymbol{x}) = \boldsymbol{O}\right\} = \{\boldsymbol{x} = \boldsymbol{O}\},\end{cases} \tag{37}$$

then $\dot{H}(\boldsymbol{x}) \leq 0$, indicating that the storage function $H(\boldsymbol{x})$ serves as a Lyapunov function. Consequently, by LaSalle's invariance principle, the system's trajectories asymptotically converge to the origin, implying

asymptotic stability of the desired steady-state.

This control design is rooted in the PH representation of the reactor dynamics. Within this structure, the storage function $H(\boldsymbol{x})$ not only serves as a Lyapunov function but also satisfies the dissipation inequality in the PH framework. The passivity condition is enforced by designing the control input to ensure that $\dot{H}(\boldsymbol{x}) \leq 0$, thereby preventing net energy injection into the system and leading to guaranteed asymptotic stability through LaSalle's invariance principle.

3. Passivity-based control of methane steam reforming

Methane is mixed with a controlled amount of steam based on the chosen steam-to-carbon molar ratio after being pressurized and heated, and then fed to the chemical reactor. In the reactor, methane and steam react over high-temperature catalysts via the following reaction,

$$CH_4 + H_2O \leftrightarrow CO + 3H_2 \quad \Delta H_{MSR} = 206\text{kJ/mol}. \tag{38}$$

From (2) and (3), the reaction rate is given as

$$r_{MSR} = k_f(T)\frac{N_{CH_4}}{V}\frac{N_{H_2O}}{V} - k_r(T)\frac{N_{CO}}{V}\frac{N_{H_2}^3}{V^3}. \tag{39}$$

The reformer can be characterized by the following equations given by the mass balance and energy balance equations from (10),

$$\begin{cases} \dot{N}_{CH_4} = \dot{n}_{CH_4,in} - N_{CH_4}/\tau - r_{MSR}V, \\ \dot{N}_{H_2O} = \dot{n}_{H_2O,in} - N_{H_2O}/\tau - r_{MSR}V, \\ \dot{N}_{CO} = -N_{CO}/\tau + r_{MSR}V, \\ \dot{N}_{H_2} = -N_{H_2}/\tau + 3r_{MSR}V, \\ \dot{T} = C_{fin}T_{in}/C_p - C_fT/C_p - \Delta H_{MSR}r_{MSR}V/C_p + \dot{Q}/C_p. \end{cases} \tag{40}$$

Let $N_{i,0}$ be the steady-state values of the mole number of species i, $\dot{n}_{CH_4,in0}$ and $\dot{n}_{H_2O,in0}$ are the feed mole numbers at the steady state, T_0, $r_{MSR,0}$ and $\dot{Q}_0$ be the steady-state values of the reactor temperature, reaction rate, and the external heat supplied to the reactor. The inlet temperature of the feed is constant.

Let $\delta\dot{n}_{CH_4,in} = \dot{n}_{CH_4,in} - \dot{n}_{CH_4,in0}, \delta\dot{n}_{H_2O,in} = \dot{n}_{H_2O,in} - \dot{n}_{H_2O,in0}, \delta N_i = N_i - N_{i0}, \delta T = T - T_0, \delta\dot{Q} = \dot{Q} - \dot{Q}_0$, the dynamic model using deviations is shown by,

$$\begin{cases} \delta\dot{N}_{CH_4} = \delta\dot{n}_{CH_4,in} - \delta N_{CH_4}/\tau - \delta r_{MSR}V, \\ \delta\dot{N}_{H_2O} = \delta\dot{n}_{H_2O,in} - N_{H_2O}/\tau - \delta r_{MSR}V, \\ \delta\dot{N}_{CO} = -\delta N_{CO}/\tau + \delta r_{MSR}V, \\ \delta\dot{N}_{H_2} = -\delta N_{H_2}/\tau + 3\delta r_{MSR}V, \\ \delta\dot{T} = -C_f\delta T/C_p - \Delta H_{rxn}\delta r_{MSR}V/C_p + \delta\dot{Q}/C_p. \end{cases} \tag{41}$$

At equilibrium points the reaction rate $r_{MSR,0}$ equals zero, however, any deviation in concentrations or temperature will cause the reaction rate to deviate from zero. To account for the deviations of the temperature and concentrations, the reaction rate deviation δr_{MSR} is given below,

$$\delta r_{MSR} = \sum_i (\partial r_{MSR}/\partial N_i)_0 \delta N_i + (\partial r_{MSR}/\partial T)_0 \delta T, \tag{42}$$

where

$$\sum_i (\partial r_{MSR}/\partial N_i)_0 \delta N_i = k_f(T_0)\left(\frac{N_{CH_4}}{V^2}\delta N_{CH_4} + \frac{N_{H_2O}}{V^2}\delta N_{H_2O} - \frac{N_{H_2}^3}{K_{eq}(T_0)V^4}\delta N_{CO} - \frac{3N_{CO}N_{H_2}^3}{K_{eq}(T_0)V^4}\delta N_{H_2}\right), \tag{43}$$

and

$$(\partial r_{MSR}/\partial T)_0 \delta T = \frac{k_f(T_0)}{RT_0^2}\frac{N_{CH_4,0}}{V}\frac{N_{H_2O,0}}{V}\Delta H_{MSR}\delta T. \tag{44}$$

Taking the state vector $\boldsymbol{x}$, the control input $\boldsymbol{u}$ and the output $\boldsymbol{y}$ as follows,

$$\boldsymbol{x} = \begin{bmatrix} \delta N_{CH_4} & \delta N_{H_2O} & \delta N_{CO} & \delta N_{H_2} & \delta T \end{bmatrix}^T, \tag{45}$$

$$\boldsymbol{u} = \begin{bmatrix} \delta\dot{n}_{CH_4,in} & \delta\dot{n}_{H_2O,in} & \delta\dot{Q} \end{bmatrix}^T, \tag{46}$$

$$\boldsymbol{y} = \begin{bmatrix} \delta N_{CO} & \delta N_{H_2} & \delta T \end{bmatrix}^T, \tag{47}$$

the nonlinear state-space model for the dynamic characteristics of the chemical reactor can be given as

$$\begin{cases} \dot{\boldsymbol{x}} = \boldsymbol{f}(\boldsymbol{x}) + \boldsymbol{G}\boldsymbol{u}, \\ \boldsymbol{y} = \boldsymbol{h}(\boldsymbol{x}), \end{cases} \tag{48}$$

$$\boldsymbol{f}(\boldsymbol{x}) = \begin{bmatrix} -x_1/\tau - \delta r_{MSR}(x)V \\ -x_2/\tau - \delta r_{MSR}(x)V \\ -x_3/\tau + \delta r_{MSR}(x)V \\ -x_4/\tau + 3\delta r_{MSR}(x)V \\ -C_fx_5/C_p - \Delta H_{rxn}\delta r_{MSR}(x)V/C_p \end{bmatrix}, \tag{49}$$

where

$$\delta r_{MSR}(x)V = k_f(T_0)\left(\frac{N_{H_2O,0}}{V}x_1 + \frac{N_{CH_4,0}}{V}x_2 - \frac{N^3{}_{H_2,0}}{K_{eq}(T_0)V^3}x_3 - \frac{3N_{CO,0}N^2{}_{H_2,0}}{K_{eq}(T_0)V^3}x_4 + \frac{N_{CH_4,0}N_{H_2O,0}\Delta H_{MSR}}{RT_0^2V}x_5\right),$$

and

$$\boldsymbol{G} = \begin{bmatrix} 1 & 0 & 0 & 0 & 0 \\ 0 & 1 & 0 & 0 & 0 \\ 0 & 0 & 0 & 0 & 1/C_p \end{bmatrix}^T. \tag{50}$$

Proposition 1. *The MSR reactor dynamics is passive when the storage function $H(\boldsymbol{x})$ is chosen as the function defined in* (22).

Proof Considering the storage function of the chemical reactor given by

$$H(\boldsymbol{x}) = \frac{1}{2}\boldsymbol{x}_c^T\boldsymbol{U}\boldsymbol{x}_c + \frac{c_v}{2T}x_5^2, \tag{51}$$

and $H(\boldsymbol{x})$ is strictly positive definite under conditions (18)–(20), the reactor dynamics (48) can be represented in the PH form,

$$\dot{\boldsymbol{x}} = [\boldsymbol{J}(\boldsymbol{x}) - \boldsymbol{R}(\boldsymbol{x})]\nabla H(\boldsymbol{x}) + \boldsymbol{G}\boldsymbol{u}, \tag{52}$$

where

$$\boldsymbol{R}(\boldsymbol{x})=\begin{bmatrix}\frac{1}{\tau}\boldsymbol{U}^{-1} & 0\\ 0 & \frac{T}{c_v}\left(\frac{C_f}{C_p}+\left(\frac{\Delta H_{MSR}}{C_p}+2\right)\frac{\delta r_{MSR}(\boldsymbol{x})V}{x_5}\right)\end{bmatrix}\quad i=1,\ldots,4, \tag{53}$$

$$\boldsymbol{J}(\boldsymbol{x})=\begin{bmatrix}0 & 0 & 0 & 0 & J_{15}\\ 0 & 0 & 0 & 0 & J_{25}\\ 0 & 0 & 0 & 0 & J_{35}\\ 0 & 0 & 0 & 0 & J_{45}\\ -J_{15} & -J_{25} & -J_{35} & -J_{45} & 0\end{bmatrix}, \tag{54}$$

$$J_{i5}=\begin{cases}\dfrac{\nu_i T\delta r_{MSR}(\boldsymbol{x})V}{c_v x_5}, x_5\neq 0\\ 0, \quad x_5=0\end{cases} \tag{55}$$

$$\nabla H(\boldsymbol{x})=\begin{bmatrix}\boldsymbol{U}\boldsymbol{x}_c & \dfrac{c_v}{T}x_5\end{bmatrix}^{\mathrm{T}}. \tag{56}$$

Since the MSR reaction is an endothermic reaction, $\Delta H_{MSR}>0$. Meanwhile, an increase in temperature leads to an increase in the reaction rate, while a decrease in temperature leads to a decrease in the reaction rate. Therefore, $\delta r_{MSR}(\boldsymbol{x})$ has the same sign as x_5. And according to condition (19), $\boldsymbol{U}:=\left[\mu_{ij}\right]>\boldsymbol{O}$, consequently, the matrix $\boldsymbol{R}(\boldsymbol{x})$ is positive definite.

For the reactor dynamics in PH form (52), the ROC of the storage function along the system trajectories satisfies

$$\begin{aligned}\dot{H}(\boldsymbol{x}) &= -\nabla H(\boldsymbol{x})^{\mathrm{T}}\boldsymbol{R}(\boldsymbol{x})\nabla H(\boldsymbol{x})+\nabla H(\boldsymbol{x})^{\mathrm{T}}\boldsymbol{G}\boldsymbol{u}\\ &= -\nabla H(\boldsymbol{x})^{\mathrm{T}}\boldsymbol{R}(\boldsymbol{x})\nabla H(\boldsymbol{x})+\boldsymbol{u}^{\mathrm{T}}\boldsymbol{y}.\end{aligned} \tag{57}$$

Since $\boldsymbol{R}(\boldsymbol{x})$ is positive definite,

$$\dot{H}(\boldsymbol{x})\leq \boldsymbol{u}^{\mathrm{T}}\boldsymbol{y}, \tag{58}$$

the system dynamics is strictly passive.

Proposition 2. *Design the control input in the PH form*(52) *satisfying the following control law*

$$\boldsymbol{u}=-\boldsymbol{K}\boldsymbol{y}, \tag{59}$$

where $\boldsymbol{K}=\mathrm{diag}(k_{11}, k_{22}, k_{55})$, and the gains k_{ii} are positive constants. The closed-loop system is globally asymptotically stable at $\boldsymbol{x}=\boldsymbol{O}$.

Proof Consider the reactor dynamics written in the PH form with output $\boldsymbol{y}=\boldsymbol{G}(\boldsymbol{x})^{\mathrm{T}}\nabla H(\boldsymbol{x})$, the ROC of the storage function along the closed-loop system trajectories satisfies

$$\begin{aligned}\dot{H}(\boldsymbol{x}) &= -\nabla H(\boldsymbol{x})^{\mathrm{T}}\boldsymbol{R}(\boldsymbol{x})\nabla H(\boldsymbol{x})+\nabla H(\boldsymbol{x})^{\mathrm{T}}\boldsymbol{G}\boldsymbol{u}\\ &= -\nabla H(\boldsymbol{x})^{\mathrm{T}}\boldsymbol{R}(\boldsymbol{x})\nabla H(\boldsymbol{x})-\nabla H(\boldsymbol{x})^{\mathrm{T}}\boldsymbol{G}\boldsymbol{K}\boldsymbol{G}^{\mathrm{T}}\nabla H(\boldsymbol{x})\\ &= -\nabla H(\boldsymbol{x})^{\mathrm{T}}\boldsymbol{R}(\boldsymbol{x})\nabla H(\boldsymbol{x})-\boldsymbol{y}^{\mathrm{T}}\boldsymbol{K}\boldsymbol{y},\end{aligned} \tag{61}$$

since $\boldsymbol{R}(\boldsymbol{x})$ and the gain matrix $\boldsymbol{K}$ is positive definite, therefore

$$\dot{H}(\boldsymbol{x})=-\nabla H(\boldsymbol{x})^{\mathrm{T}}\boldsymbol{R}(\boldsymbol{x})\nabla H(\boldsymbol{x})-\boldsymbol{y}^{\mathrm{T}}\boldsymbol{K}\boldsymbol{y}\leq 0. \tag{62}$$

The ROC of the storage function equals to zero when $\nabla H(\boldsymbol{x})=\boldsymbol{0}$ and $\boldsymbol{y}=\boldsymbol{0}$. Since $\boldsymbol{y}=\boldsymbol{G}^{\mathrm{T}}\nabla H(\boldsymbol{x})$, and matrix G is full rank, then $\boldsymbol{y}=\boldsymbol{0}$ implies $\nabla H(\boldsymbol{x})=\boldsymbol{0}$. Given that the storage function is positive definite, $\nabla H(\boldsymbol{x})=\boldsymbol{0}$ if and only if $\boldsymbol{x}=\boldsymbol{O}$, it follows that the largest invariant set where $\dot{H}(\boldsymbol{x})=0$ is at the origin $\boldsymbol{x}=\boldsymbol{O}$. According to LaSalle's invariance principle, the closed-loop system is globally asymptotically stable at the desired equilibrium point $\boldsymbol{x}=\boldsymbol{O}$. The control structure implementing the proposed passivity-based control law is schematically illustrated in Fig. 1.

4. Application to a nuclear hydrogen cogeneration plant

The control is applied to regulate the reformer in a nuclear hydrogen production plant based on the multi-modular high-temperature gas-cooled reactor (HTGR). The simulation is conducted using the HTR-PM600 dynamics simulation software [30] with the MSR reaction kinetics modeled in Refs. [31–33]. The schematic diagram of the plant is shown in Fig. 2. The steam produced from the nuclear power plant is heated by an electrical heater to a higher temperature, then heated the reformer for hydrogen production. After that the used steam is used for electricity generation in turbine sets. Table 1 shows the steady-state conditions of the cogeneration plant.

This additional heating step is essential to meet the reaction temperature requirement of approximately 700 °C for the MSR reactor. The electrical power used for this reheating process is supplied by the nuclear power plant's own power generation system, ensuring internal energy self-sufficiency within the cogeneration system. This approach avoids the combustion of additional methane for reformer heating, thereby reducing carbon emissions and enhancing the sustainability of the system. Furthermore, the cogeneration strategy improves the economic efficiency of the nuclear plant by enabling simultaneous electricity and hydrogen production, making full use of the thermal output. The feasibility of this reheating configuration has been demonstrated in previous studies [33], and this modeling assumption is accordingly adopted in this study. In particular, the main steam heating configuration follows the validated HTR-PM600 dynamics software [29], and the operational conditions for the MSR reformer are based on industrially representative steady-state parameters, which have been verified against real-world data in previous studies [34,35].

To validate the effectiveness of the proposed passivity-based control strategy, this section presents the application of the designed controller to the MSR reactor under two representative simulation scenarios. Control signals u_1 and u_2 adjust the inlet flowrate of methane and steam, respectively, while u_3 adjust the power of the electrical heater that heats the steam from NSSSs.

The reactor model adopts the port-Hamiltonian formulation described earlier, and the control law follows the structure proposed in Proposition 2, with gain values $k_{11}=k_{22}=3$, and $k_{55}=1.7\times 10^5$. The nominal operating point corresponds to an inlet methane flow of 1000 mol/s with a steam-to-carbon ratio of 3.2.

1) Response Under Different Initial Conditions

The reformer closed-loop responses of different initial conditions shown in Table 2 are presented in this section.

The simulation results provide critical insights into the effectiveness

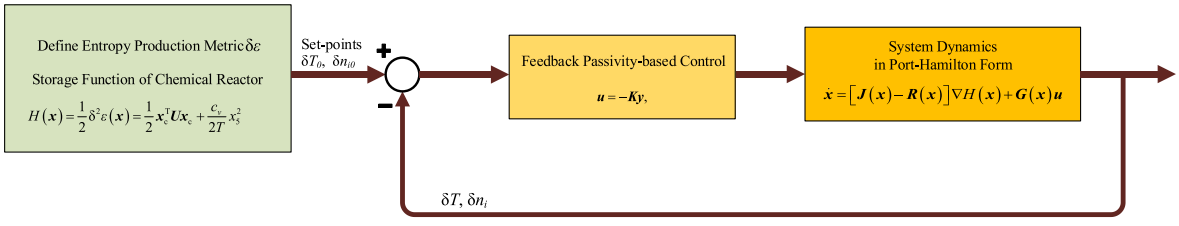

Fig. 1. Schematic diagram of the passivity-based control.

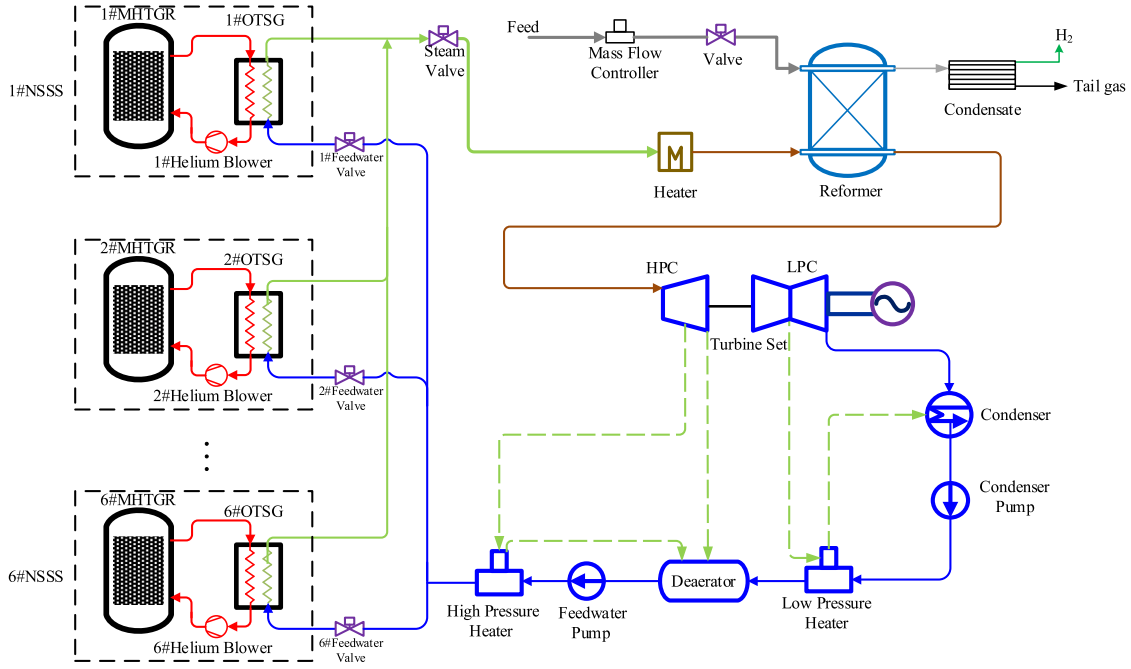

Fig. 2. Schematic diagram of the nuclear hydrogen production plant based on HTGR.

Table 1
Steady-state conditions of the cogeneration plant at full power.

	Value	Unit
Plant thermal power	1500	MW
Hydrogen production	6.12	metric ton/h
Electricity generation	780.7	MW
Main steam temperature	560	°C
Main steam pressure	13.24	MPa
Main steam flowrate	605	kg/s
Hydrogen production pressure	1	MPa
MSR reaction temperature	700	°C
Electrical heater power	386.1	MW

Table 2
Initial conditions for simulations.

Symbol/unit	C_1	C_2	C_3	C_4
$T(0)$/°C	701.7	901.1	698.6	697.2
$N_1(0)$/mol	36	35.3	34.1	33.8
$N_2(0)$/mol	543.6	542.9	541.7	541.3
$N_3(0)$/mol	196.9	196.7	195.4	194.6
$N_4(0)$/mol	590.9	589.9	586.4	584.2

of the PBC framework for the reformers. The responses of key variables shown in Figs. 3–8, including the reactor temperature and the mole number of CH_4, H_2O, CO, and H_2, demonstrate that the control design achieves stable and efficient operation under disturbances. The transient behaviors indicate that the system effectively compensates for perturbations. The closed-loop responses exhibit less than 1 % overshoot and reach steady state within approximately 50 s, indicating adequate dynamic performance. Despite sudden changes, the system stabilizes quickly, maintaining thermodynamic consistency and ensuring energy-efficient operation. These results validate the ability of the proposed PBC to handle the coupled dynamics and nonlinearities inherent in the MSR process.

The convergence of the key parameters to the desired steady states shows that the controller is designed such that the closed-loop system's eigenvalues possess sufficiently negative real parts. Fig. 8 show that the

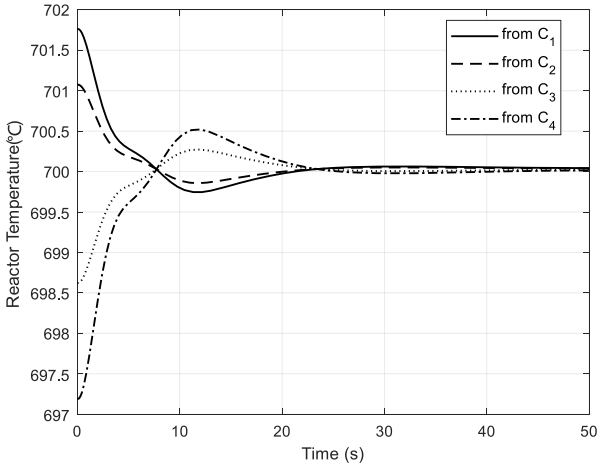

Fig. 3. Closed-loop responses of the reformer temperature.

ROC of the storage function $H(\boldsymbol{x})$ is negative definite and converges to zero. The transient oscillations observed in $\nabla H(\boldsymbol{x})$ are directly attributable to the complex eigenvalues of the closed-loop system. Despite these oscillations, the ROC remains negative definite, ensuring that the storage function decreases over time and the system states converge to the origin.

2) Response Under Reactor Load Disturbances

In order to further verify the applicability of the proposed control method under realistic operational scenarios, this subsection investigates the reformer system's behavior when subject to reactor load disturbances. The simulation considers a load reduction scenario in the HTR-PM600 cogeneration system, where one of the six reactor modules undergoes a linear 50 % power drop starting from the 20,000th second, while the remaining modules maintain nominal power.

When the reactor load changes, the main steam system maintains the pressure and temperature close to their setpoints through reactor power

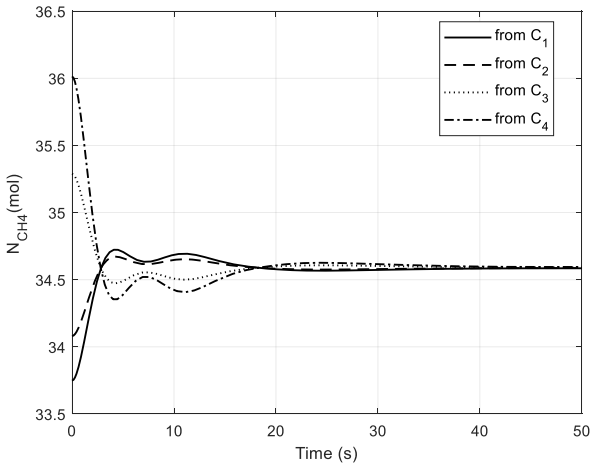

Fig. 4. Closed-loop responses of N_1.

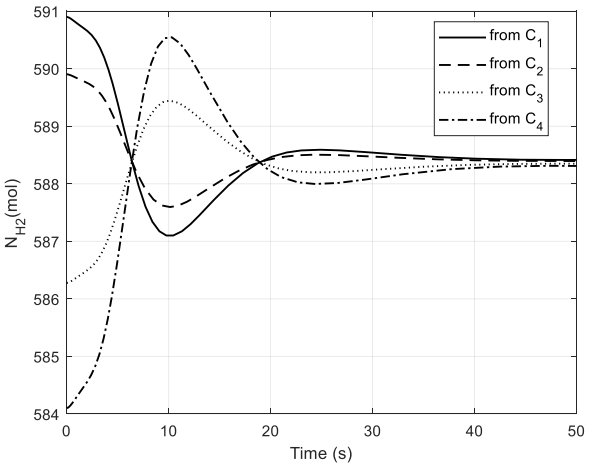

Fig. 7. Closed-loop responses of N_4.

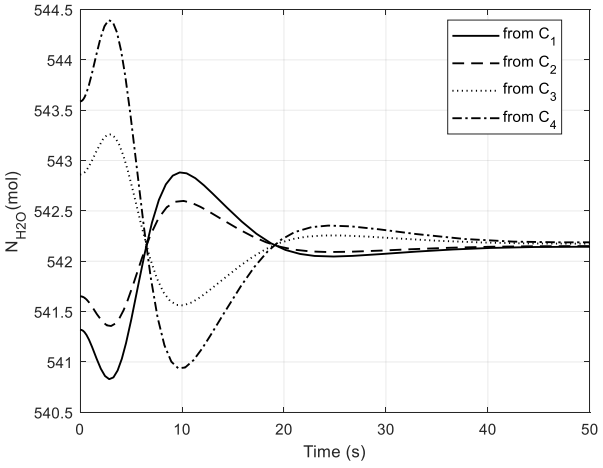

Fig. 5. Closed-loop responses of N_2.

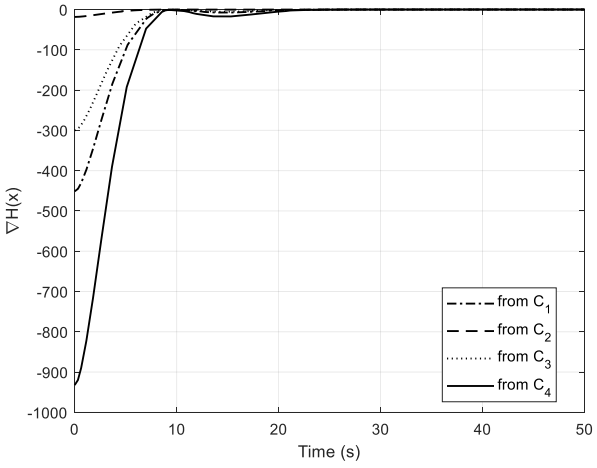

Fig. 8. ROC of the storage function along the dynamics of the system.

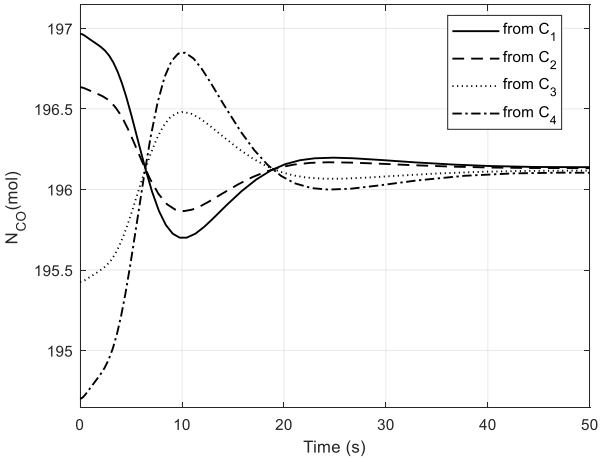

Fig. 6. Closed-loop responses of N_3.

control while a noticeable reduction in the steam flowrate occurs. Since the MSR reactor relies on steam from the NSSS as its heat source, this reduction in steam flow leads to a perturbation in the MSR reactor states, which subsequently activates the control response. Fig. 9 illustrates the closed-loop responses of the MSR reactor under the load change. A comparison is also made between the proposed passivity-based controller (PBC) and a conventional PI controller. The proportional gains in the PI controller are set equal to those in the PBC, and the integral gains are fixed at 10. As shown in the figure, the PBC demonstrates a better performance in regulating the reactor temperature and mole numbers (e.g., CO and H_2).

Moreover, it can be observed that the temperature controller plays a dominant role in the overall control scheme, significantly influencing the system's dynamic behavior. This dominance stems from the considerably higher control gain assigned to the temperature control channel ($k_{55} = 1.7 \times 10^5$), compared to the flowrate control gains ($k_{11} = k_{22} = 3$). By prioritizing temperature regulation, the design indirectly stabilizes other state variables. The proposed PBC not only achieves robust temperature control but also enables coordinated regulation of the mole numbers of multiple chemical species, demonstrating its effectiveness in managing multi-input multi-output systems such as the MSR reactor.

A key advantage of the PBC approach is its reliance on a

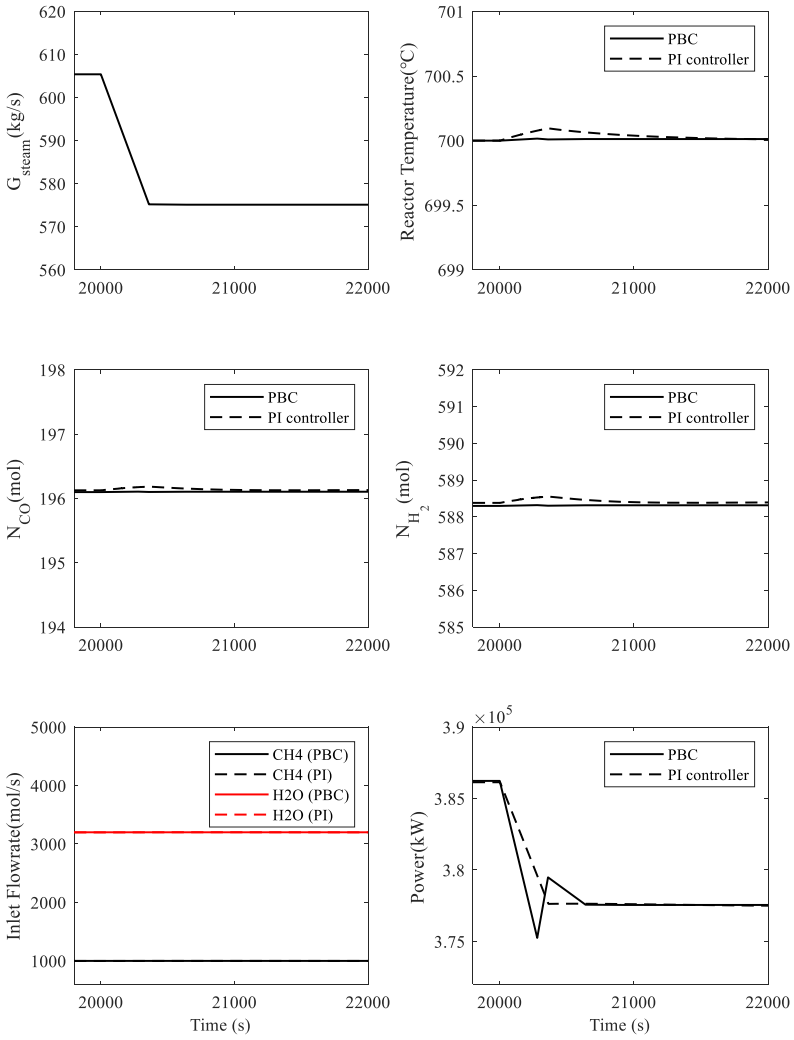

Fig. 9. System responses under reactor load reduction.

thermodynamically consistent storage function, incorporating entropy production metrics to ensure passivity. The practical implications of these findings are significant, particularly for hydrogen production within nuclear cogeneration systems. The ability to stabilize MSR reactors under dynamic conditions ensures consistent hydrogen output, contributing to the reliability and efficiency of integrated energy systems. Future work could explore the extension of this control framework to multi-phase systems or more complex reactor designs to further enhance its applicability.

5. Conclusions

This study has developed a comprehensive PBC framework for MSR reactors, addressing the critical challenges posed by the nonlinear and thermodynamically complex dynamics of the system. By formulating a deviation-based dynamic model and incorporating a thermodynamically consistent storage function grounded in entropy production metrics, the proposed method ensures stability and energy-efficient operation. The control design appropriately shaping the system's energy properties and ensuring passivity and is validated through application to a hydrogen production plant within a modular high-temperature gas-cooled reactor system, demonstrating its practical relevance and effectiveness under operational disturbances. The control law is convenient for practical implemented. The results highlight effectiveness in maintaining system stability and operational efficiency, providing a pathway for broader adoption of PBC in other thermodynamically governed chemical processes. Future work will focus on extending the application of this framework to other reactors in the hydrogen production system and exploring its integration with advanced reactor designs to further optimize hydrogen production and energy sustainability.

CRediT authorship contribution statement

Junyi Li: Writing – original draft, Methodology, Formal analysis, Conceptualization. **Zhe Dong:** Writing – review & editing, Validation, Supervision, Software, Project administration.

Declaration of competing interest

The authors declare that they have no known competing financial interests or personal relationships that could have appeared to influence the work reported in this paper.

Appendix A. Supplementary data

Supplementary data to this article can be found online at https://doi.org/10.1016/j.ijhydene.2025.05.367.

References

[1] Møller KT, Jensen TR, Akiba E, Li H-w. Hydrogen - a sustainable energy carrier. Prog Nat Sci Mater Int 2017/02/01/2017;27(1):34–40. https://doi.org/10.1016/j.pnsc.2016.12.014.

[2] Hosseini SE. Chapter 1 - hydrogen, a green energy carrier. In: Hosseini SE, editor. Fundamentals of hydrogen production and utilization in fuel cell systems. Elsevier; 2023. p. 1–37.

[3] Ighalo JO, Amama PB. Recent advances in the catalysis of steam reforming of methane (SRM). Int J Hydrogen Energy 2024/01/02/2024;51:688–700. https://doi.org/10.1016/j.ijhydene.2023.10.177.

[4] Zhang K-R, Tang X-Y, Yang W-W, Li J-C, Zhang R-Z. Back propagation neural network based proportional-integral hybrid control strategy for a solar methane reforming reactor. Int J Hydrogen Energy 2024/01/02/2024;49:1258–71. https://doi.org/10.1016/j.ijhydene.2023.09.215.

[5] Lao L, Aguirre A, Tran A, Wu Z, Durand H, Christofides PD. CFD modeling and control of a steam methane reforming reactor. Chem Eng Sci 2016/07/12/2016;148:78–92. https://doi.org/10.1016/j.ces.2016.03.038.

[6] Medjebouri A. Extended state observer based robust feedback linearization control applied to an industrial CSTR. J Autom Mobile Robot Intelligent Syste 2024;17(4):68–78. https://doi.org/10.14313/jamris/4-2023/32.

[7] Zecevic N, Bolf N. Advanced operation of the steam methane reformer by using gain-scheduled model predictive control. Ind Eng Chem Res 2020/02/26 2020;59(8):3458–74. https://doi.org/10.1021/acs.iecr.9b06260.

[8] Alhajeri MS, Ren YM, Ou F, Abdullah F, Christofides PD. Model predictive control of nonlinear processes using transfer learning-based recurrent neural networks. Chem Eng Res Des 2024/05/01/2024;205:1–12. https://doi.org/10.1016/j.cherd.2024.03.019.

[9] Lee J, et al. Machine learning-based energy optimization for on-site SMR hydrogen production. Energy Convers Manag 2021/09/15/2021;244:114438. https://doi.org/10.1016/j.enconman.2021.114438.

[10] Afanasev P, et al. An overview of hydrogen production methods: focus on hydrocarbon feedstock. Int J Hydrogen Energy 2024/08/12/2024;78:805–28. https://doi.org/10.1016/j.ijhydene.2024.06.369.

[11] From TN, et al. Electrified steam methane reforming of biogas for sustainable syngas manufacturing and next-generation of plant design: a pilot plant study. Chem Eng J (Amsterdam, Neth) 2024/01/01/2024;479:147205. https://doi.org/10.1016/j.cej.2023.147205.

[12] Çıtmacı B, et al. Model predictive control of an electrically-heated steam methane reformer. Digital Chem Eng 2024/03/01/2024;10:100138. https://doi.org/10.1016/j.dche.2023.100138.

[13] Çıtmacı B, et al. Feedback control of an experimental electrically-heated steam methane reformer. Chem Eng Res Des 2024/06/01/2024;206:469–88. https://doi.org/10.1016/j.cherd.2024.05.021.

[14] Yang W-W, Yang Y-J, Tang X-Y, Zhang K-R, Li J-C, Xu C. An adaptive P/PI control strategy for a solar volumetric methane/steam reforming reactor with passive thermal management. Chem Eng Sci 2023/11/05/2023;281:119005. https://doi.org/10.1016/j.ces.2023.119005.

[15] Wang Y, et al. Machine learning-based predictive control of an electrically-heated steam methane reforming process. Digital Chem Eng 2024/09/01/2024;12:100173. https://doi.org/10.1016/j.dche.2024.100173.

[16] Cai Z, Ydstie BE. Passivity of single-phase thermodynamic systems with equilibrium reactions. IFAC-PapersOnLine 2022/01/01/2022;55(7):248–53. https://doi.org/10.1016/j.ifacol.2022.07.452.

[17] Zhou W, Hamroun B, Le Gorrec Y, Couenne F. A thermodynamic approach to the stabilization of tubular reactors. J Process Control 2021/12/01/2021;108:98–111. https://doi.org/10.1016/j.jprocont.2021.11.006.

[18] Hoang NH, Couenne F, Jallut C, Le Gorrec Y. Thermodynamics based stability analysis and its use for nonlinear stabilization of the CSTR. Comput Chem Eng 2013/11/11/2013;58:156–77. https://doi.org/10.1016/j.compchemeng.2013.06.016.

[19] van der Schaft A, Jeltsema D. Port-Hamiltonian systems theory: an introductory overview. Foundat Trends® in Syste Control 2014;1(2–3):173–378. https://doi.org/10.1561/2600000002.

[20] Duindam V, Macchelli A, Stramigioli S, Bruyninckx H. Port-Hamiltonian systems. In: Duindam V, Macchelli A, Stramigioli S, Bruyninckx H, editors. Modeling and control of complex physical systems: the port-Hamiltonian approach. Berlin, Heidelberg: Springer Berlin Heidelberg; 2009. p. 53–130.

[21] Philipp FM, Schaller M, Worthmann K, Faulwasser T, Maschke B. Optimal control of port-Hamiltonian systems: energy, entropy, and exergy. Syst Control Lett 2024/12/01/2024;194:105942. https://doi.org/10.1016/j.sysconle.2024.105942.

[22] Ha Hoang N, Couenne F, Le Gorrec Y, Chen CL, Ydstie BE. Passivity-based nonlinear control of CSTR via asymptotic observers. Annu Rev Control 2013/12/01/2013;37(2):278–88. https://doi.org/10.1016/j.arcontrol.2013.09.007.

[23] Ramírez H, Le Gorrec Y, Maschke B, Couenne F. On the passivity based control of irreversible processes: a port-Hamiltonian approach. Automatica 2016/02/01/2016;64:105–11. https://doi.org/10.1016/j.automatica.2015.07.002.

[24] Hoang H, Couenne F, Jallut C, Le Gorrec Y. The port Hamiltonian approach to modeling and control of Continuous Stirred Tank Reactors. J Process Control 2011/12/01/2011;21(10):1449–58. https://doi.org/10.1016/j.jprocont.2011.06.014.

[25] Hoang NH, Ydstie BE. Integration of inventory control into the port-Hamiltonian framework for dissipative stabilization of chemical reactors. Asian J Control 2022/09/01 2022;24(5):2490–504. https://doi.org/10.1002/asjc.2668.

[26] Dong Z, Li J, Zhang Z, Dong Y, Huang X. The definition of entropy production metric with application in passivity-based control of thermodynamic systems. Renew Sustain Energy Rev 2025/03/01/2025;209:115065. https://doi.org/10.1016/j.rser.2024.115065.

[27] Xing L. Yan SK, Hori Masao, Ryutaro Hino. Nuclear hydrogen production: an overview. 2011. https://doi.org/10.1201/b10789.

[28] Şahin S, Şahin HM. Generation-IV reactors and nuclear hydrogen production. Int J Hydrogen Energy 2021/08/18/2021;46(57):28936–48. https://doi.org/10.1016/j.ijhydene.2020.12.182.

[29] Dong Z, Pan Y, Zhang Z, Dong Y, Huang X. Dynamical modeling and simulation of the six-modular high temperature gas-cooled reactor plant HTR-PM600. Energy (Calg) 2018/07/15/2018;155:971–91. https://doi.org/10.1016/j.energy.2018.05.056.

[30] Xu J, Froment GF. Methane steam reforming, methanation and water-gas shift: I. Intrinsic kinetics. AIChE J 1989;35(1):88–96.

[31] De Falco M, Piemonte V, Di Paola L, Basile A. Methane membrane steam reforming: heat duty assessment. Int J Hydrogen Energy 2014/03/18/2014;39(9):4761–70. https://doi.org/10.1016/j.ijhydene.2013.09.066.

[32] Hou K, Hughes R. The kinetics of methane steam reforming over a Ni/α-Al2O catalyst. Chem Eng J (Amsterdam, Neth) 2001/03/15/2001;82(1):311–28. https://doi.org/10.1016/S1385-8947(00)00367-3.

[33] Li J, Dong Z, Li B, Huang X. Dynamic modeling of nuclear hydrogen generation plant based on multi-modular high-temperature gas-cooled reactor. 2022 29th international conference on nuclear engineering, 15. Student Paper Competition; 2022. https://doi.org/10.1115/ICONE29-88899.

[34] Boyano A, Blanco-Marigorta AM, Morosuk T, Tsatsaronis G. Exergoenvironmental analysis of a steam methane reforming process for hydrogen production. Energy (Calg) 2011/04/01/2011;36(4):2202–14. https://doi.org/10.1016/j.energy.2010.05.020.

[35] Simpson AP, Lutz AE. Exergy analysis of hydrogen production via steam methane reforming. Int J Hydrogen Energy 2007/12/01/2007;32(18):4811–20. https://doi.org/10.1016/j.ijhydene.2007.08.025.